Am J Physiol Heart Circ Physiol
280: H1320–H1334, 2000.

Myofibrillar disruption in hypocontractile myocardium showing perfusion-contraction matches and mismatches

ANDREW J. SHERMAN,[1,3] FRANCIS J. KLOCKE,[1,2] ROBERT S. DECKER,[1,2,5] MARLENE L. DECKER,[1] KAREN A. KOZLOWSKI,[1] KATHLEEN R. HARRIS,[1] SASCHA HEDJBELI,[1] YURI YAROSHENKO,[1] SAKIE NAKAMURA,[1] MICHELE A. PARKER,[1] PAUL A. CHECCHIA,[4] AND DANIEL B. EVANS[1]
[1]*Feinberg Cardiovascular Research Institute and the Departments of* [2]*Medicine,* [3]*Surgery,* [4]*Pediatrics, and* [5]*Cell and Molecular Biology, Northwestern University Medical School, Chicago, Illinois 60611-3008*

Sherman, Andrew J., Francis J. Klocke, Robert S. Decker, Marlene L. Decker, Karen A. Kozlowski, Kathleen R. Harris, Sascha Hedjbeli, Yuri Yaroshenko, Sakie Nakamura, Michele A. Parker, Paul A. Checchia, and Daniel B. Evans, Myofibrillar disruption in hypocontractile myocardium showing perfusion-contraction matches and mismatches. *Am J Physiol Heart Circ Physiol* 280: H1320–H1334, 2000.—Chronically instrumented dogs underwent 2- or 5-h regional reductions in coronary flow that were followed, respectively, by balanced reductions in myocardial contraction and O_2 consumption ("hibernation") and persistently reduced contraction despite normal myocardial O_2 consumption ("stunning"). Previously unidentified myofibrillar disruption developed during flow reduction in both experimental models and persisted throughout the duration of reperfusion (2–24 h). Aberrant perinuclear aggregates that resembled thick filaments and stained positively with a monoclonal myosin antibody were present in 34 ± 3.8% (SE) and 68 ± 5.9% of "hibernating" and "stunned" subendocardial myocytes in areas subjected to flow reduction and in 16 ± 2.5% and 44 ± 7.4% of subendocardial myocytes in remote areas of the same ventricles. Areas of myofibrillar disruption also showed glycogen accretion and unusual heterochromatin clumping adjacent to the inner nuclear envelope. The degrees of flow reduction employed were sufficient to reduce regional myofibrillar creatine kinase activity by 25–35%, but troponin I degradation was not evident. The observed changes may reflect an early, possibly reversible, phase of the myofibrillar loss characteristic of hypocontractile myocardium in patients undergoing revascularization.

myocardial hibernation; stunning; apoptosis; stress proteins; myocardial ischemia

CONTINUING INTEREST in the characterization of viable, reversibly hypocontractile myocardium as "hibernating" or "stunned" reflects the importance as well as the difficulty in distinguishing between beneficial adaptations and transient injurious responses to flow limitation. The distinction has usually been made on the basis of whether resting coronary flow (which is taken as a surrogate for myocardial O_2 consumption) is normal or reduced. "Matched" reductions in resting perfusion and function are thought to represent an adaptation that reduces susceptibility to regional ischemia, whereas perfusion-function "mismatches" are taken to represent persistent myocardial injury following a period of supply-to-demand imbalance.

Although the mechanisms underlying stunning and/or hibernation remain unsettled, a reasonably consistent pattern of structural abnormalities has been noted by several laboratories (2, 13, 58) in myocardial biopsies obtained from dysfunctional areas of the human left ventricle during coronary bypass surgery. These changes include a loss of myofibrils, the accumulation of glycogen, and variable degrees of interstitial fibrosis and are believed to represent chronic rather than acute responses to flow reduction.

Our laboratory (50) demonstrated that matched reversible reductions in systolic function and myocardial O_2 consumption meeting the criterion for hibernation occur for brief periods after moderate 2-h regional reductions in coronary flow in chronically instrumented dogs. More marked 5-h reductions in flow are known to produce the perfusion-function mismatch, which is typical of stunning (32). Using these contrasting models, the present study was undertaken to determine whether subcellular morphological changes occur in either or both of these circumstances and, if so, whether they are similar to those identified in patients. From the known limitations of acute instrumentation and open-chest preparations (25, 30, 56), studies were again performed in chronically instrumented dogs. To assist in placing morphological findings in context with related studies from other laboratories, we also assessed in situ DNA fragmentation, troponin I degradation, myofibrillar creatine kinase (CK) activity, and mRNA levels for three myocardial stress proteins.

METHODS

Studies were conducted in mongrel dogs of both sexes using procedures and protocols concordant with the "Guiding Principles in the Care and Use of Animals" endorsed by the American Physiological Society.

The costs of publication of this article were defrayed in part by the payment of page charges. The article must therefore be hereby marked "*advertisement*" in accordance with 18 U.S.C. Section 1734 solely to indicate this fact.

Experimental Preparation

Twenty-nine dogs weighing 23–36 kg were instrumented after an overnight fast and a 3-wk period of on-site conditioning. Details of the instrumentation procedure have been published previously (50). A micromanometer (Konigsberg Instruments P 6.5, Pasadena, CA) was inserted into the left ventricular cavity through the ventricular apex. The proximal portion of the left circumflex (LCx, $n = 25$) or anterior descending (LAD, $n = 4$) coronary artery was instrumented with a volumetric transit time ultrasonic flow probe (model 3RB for LCx or model 2SB for LAD, Transonics, Ithaca, NY) and a hydraulic occluder. A small plastic catheter was introduced directly into the coronary sinus (LCx dogs) or the great cardiac vein (LAD dogs). Ultrasonic crystal pairs were placed in the central portions of the distributions of the LCx and LAD beds for measurement of subendocardial segment length or wall thickness. In 18 animals left atrial and aortic catheters were also placed for fluorescent microsphere flow measurements (17). Animals were allowed to recover for 7–10 days before being studied in the unanesthetized state.

Study Procedures

Animals were studied while lightly sedated with Innovar-Vet (fentanyl 0.4 mg/ml and droperidol 20 mg/ml) and while resting in a sling to which they had previously been acclimated. As described previously (50), hemodynamic and sonomicrometric data were monitored continuously in analog (Vidco 516YT, Beaverton, OR) and digital (DataFlow, Crystal Biotech, Hopkinton, MA) form. Average values for individual parameters were calculated from digitized data sampled for 30–40 s at a rate of 180 Hz. Myocardial O_2 consumption was calculated as the product of LCx or LAD flow and the arterial-venous difference in O_2 content.

"Hibernation" model. Twelve animals were studied using sustained 2-h reductions in regional flow sufficient to cause an ~50% reduction in regional systolic segment shortening or wall thickening. To minimize variations in hemodynamics, heart rate was maintained constant using atrial pacing (AAI pacing). Partial coronary artery occlusions were applied gradually by injecting saline into the hydraulic occluder in increments of 2–10 μl over ~20 min until the desired level of segmental function was reached. The partial occlusion was then maintained for 2 h, with adjustment as needed to keep segmental function at the desired level. Microsphere measurements were performed before and near the midpoint of the period of occlusion. Five animals were euthanized (without reperfusion) at the end of the 2-h period of reduced flow. The remaining seven animals underwent reperfusion for 2 h before death. Euthanasia was performed with an overdose of pentobarbital sodium and potassium chloride.

"Stunning" model. Ten animals were studied using sustained 5-h reductions in regional flow sufficient to reduce regional segmental function by ~75%. AAI pacing and microsphere measurements were performed as in the hibernating model. Three animals were euthanized (without reperfusion) at the completion of the 5-h period of reduced flow. The remaining seven animals were observed in the laboratory for ~1 h following the onset of reperfusion and then were returned to their cages. The following morning they were brought to the laboratory for final measurements and euthanasia.

Animals studied after recovery of function. In four dogs euthanasia was delayed until regional segmental function had returned to its baseline level on the day of flow reduction. Three animals subjected to the stunning protocol were euthanized after 2, 6, and 9 days of reperfusion, respectively. One animal subjected to the hibernating protocol was euthanized after 2 days of reperfusion.

Sham animals. Three instrumented animals were sedated in the usual fashion and euthanized without any reductions in coronary flow.

POSTMORTEM ANALYSES

The chest was opened immediately after the animal was euthanized, and transmural biopsies (1 mm in diameter) were obtained for electron microscopy from central portions of the LCx and LAD areas of the left ventricle with the heart still in situ. The heart was then removed and immersed in iced saline for further processing. Tissue from central portions of the LCx and LAD beds was subdivided into inner and outer halves: ~0.5-g specimens from each area were used for myofibril isolation, and 1–2 g inner wall segments were used for microsphere analysis. Additional samples were taken for frozen section preparation. The remainder was cut into small pieces, frozen in liquid nitrogen, and stored at −80°C.

Electron microscopy and morphometric analyses. Samples (1×2 mm) from subendocardial and subepicardial portions of each biopsy were preserved in 2% glutaraldehyde buffered in 0.1 M sodium cacodylate buffer (pH 7.4) for 12–24 h at 4°C. Specimens were postfixed and embedded in an epoxy resin as previously described (11). Thick (0.5 μm) sections were stained with 1% toluidine blue or the periodic acid-Schiff reagent (PAS) and examined with a Leitz Orthoplan phase-contrast microscope (Nuhsbaum, McHenry, IL). Thin (~50 nm) sections were stained with uranyl acetate and lead citrate and viewed and photographed with a JOEL 100CX electron microscope (JOEL, Peabody, MA).

All morphological observations were conducted in a double-blind fashion. More than 5,000 myocytes were analyzed for myofibril organization, glycogen content, mitochondrial damage, and nuclear chromatin condensation. Myofibrillar changes were evaluated using a semiquantitative scale (0 = no myofibrillar abnormalities; 1 = perinuclear myofibril disruption; 2 = myofibrillar disruption in perinuclear areas and between adjacent myofibrils; 3 = myofibrillar disruption with reduced A-band length). Data for each experimental paradigm were pooled to determine the percentage of myocytes exhibiting myofibrillar disruption. For quantitative assessment of myofibrillar organization, stereological principles were employed to determine the volume densities of intact myofibrils and disrupted myofibrils. From each experiment, eight blocks of tissue were thin sectioned. Randomly selected grid squares were photographed from each block, and electron microscopic negatives were scanned and enlarged to 10,000 times. Only cardiac myocytes were photographed; nuclei were included when present (72% of images). Volume densities of intact myofibrils and disrupted myofibrillar arrays were calculated using a rectilinear grid (11) and expressed as percentages of total myocyte volume density.

In 20 animals glycogen content also was evaluated semiquantitatively from PAS-stained sections, using a scale ranging from 0 to 3 (0 = diffuse perinuclear PAS-positive staining; 1 = discrete perinuclear deposits of PAS-positive material; 2 = bipolar perinuclear PAS-positive staining; 3 = extensive bipolar perinuclear and intermyofibrillar PAS-positive deposits).

Immunofluorescence microscopy. The distribution of myosin was evaluated in frozen sections of myocardium obtained from both models. Frozen sections (4–6 μm) were fixed in freshly prepared 4% paraformaldehyde buffered in PBS (pH 7.4) 5 min at room temperature before being rinsed in PBS (3 changes for 30 min). After the sections were blocked with normal goat serum (1:10 in PBS) overnight to minimize

nonspecific adsorption of the primary antibody, sections were incubated in a mouse monoclonal anti-myosin antibody [CCM-52, 1:500 in PBS/1% BSA (10)] for 1 h at 37°C and washed at room temperature in PBS (3 changes for 30 min). Sections were then treated with a goat anti-mouse polyclonal antibody (1:100 in PBS) labeled with fluorescein isothiocyanate to visualize the thick filament protein by epifluorescence microscopy. Some sections also were examined with a Zeiss LSM 210 laser scanning confocal microscope so that myocytes could be optically sectioned and reconstructed to gather a more complete set of images of the distribution of myosin within individual myocytes.

DNA fragmentation. In situ end labeling mediated by terminal deoxynucleotidyl transferase (TdT) was assessed in 23 animals (ApopTag kit, Oncor, Gaithersburg, MD). Deparaffinized myocardial sections (6 μm) were treated with proteinase K (20 μg/ml) and exposed to TdT enzyme and digoxigenin-labeled nucleotide (60 min at 37°C). After several washes, they were incubated with fluorescein-conjugated anti-digoxigenin antibody and then mounted with antifade mounting medium containing propidium iodide. In animals subjected to flow reduction, specimens were taken from the test and remote areas of the ventricle, and 1,000 myocyte nuclei were counted in each. In sham animals, specimens were taken from the LAD and LCx beds, and 2,000 myocyte nuclei were counted in each. The number of ApopTag-positive nuclei was expressed as percent positive.

Myofibril preparation and CK analysis. In 19 animals, myofibrils were prepared from the myocardial samples by the method of Solaro et al. (52). Protease inhibitors were present throughout the isolation procedure (leupeptin, pepstatin, and aprotinin, all 1 μg/ml). CK activity was determined using a commercial CK assay kit (Sigma).

Immunoblotting for troponin I. Frozen tissue samples were pulverized in a chilled mortar and pestle, suspended in sample lysis buffer [0.2 M dithiothreitol, 4% SDS, 0.16 M Tris·HCl (pH 6.8) and 20% glycerol], boiled at 95°C for 5 min, and centrifuged at 14,000 *g* for 5 min. Proteins were separated by 15% SDS-PAGE and electrophoretically transferred to a polyvinylidene fluoride membrane (Millipore) at 400 mA for 60 min. Sample loading and transfer efficiency were evaluated by Coomasie brilliant blue staining. The membrane was blocked overnight in a solution of 0.15 M NaCl, 0.01 M Tris (pH 8.0) and 0.05% Tween 20 (TBST) and 3% nonfat dairy milk and then incubated for 1 h with an anti-troponin I monoclonal antibody (Clone 110, Research Diagnostics). An anti-mouse IgG conjugated to horseradish peroxidase was used as a secondary antibody. Specific bands were visualized by autoradiography following incubation with a chemiluminescent substrate (Pierce). Quantification was performed with an imaging densitometer (model GS-700, Bio-Rad, Hercules, CA).

Test and remote area tissues from 9 hibernating animals (3 of which were nonreperfused), 10 stunned animals (3 nonreperfused), and 1 sham animal were studied. For the troponin I band (31 kDa), the response between densitometric signal and amount of protein loaded was linear to ~0.8 μg/lane.

mRNA levels. Total RNA was isolated from frozen inner wall myocardial samples after homogenization in acid guanidinium thiocyanate-phenol-chloroform (TRIzol, Life Technologies) in 12 animals. After Northern blotting, mRNA levels were quantified by dot-blot analysis. Heat shock protein (HSP)-70 cDNA was a gift from R. Morimoto (Northwestern University). Plasmid cDNAs for HSP-27 and α-B-crystallin were purchased commercially (Stressgen and American Type Culture Collection, respectively). A 28S cDNA probe provided by H. W. Schnaper (Northwestern University) was used for internal control and normalization.

Data Analysis

Results are presented as means ± SE. Serial hemodynamic values were assessed using paired *t*-tests and one-way ANOVA. The frequencies of myofibrillar disruption in myocardium subjected to flow reduction ("test" areas) and myocardium from normally perfused areas of the free wall of the same ventricle ("remote" areas) were analyzed in hibernating and stunned animals using three-factor ANOVA with repeated measures for a single factor (test vs. remote). Paired *t*-tests were used to compare values of glycogen score and DNA fragmentation in test and remote areas of each ventricle. Values for CK activity and mRNA levels in test areas were expressed as ratios of values in corresponding remote areas; 95% confidence limits that did not include unity were taken as statistically significant.

RESULTS

Hemodynamics

Baseline values for arterial pH, P_{CO_2}, P_{O_2}, O_2 saturation, and hemoglobin averaged 7.36 ± 0.01, 38 ± 0.7 mmHg, 89 ± 1.7 mmHg, 96 ± 1.0%, and 11.7 ± 0.3 g/dl, respectively. Values for coronary venous pH, P_{CO_2}, P_{O_2}, and O_2 saturation averaged 7.32 ± 0.01, 46 ± 1.0 mmHg, 17 ± 0.7 mmHg, and 19 ± 1.4%.

Hemodynamic and O_2 consumption data in hibernating animals undergoing flow reduction and reperfusion are presented in Table 1. During partial occlusion, regional systolic function (segment shortening or wall thickening) averaged 50 ± 2% of preocclusion values. Reductions in function were similar in animals euthanized without reperfusion (51 ± 3% of baseline). Inner wall microsphere flows averaged 54 ± 4% of preocclusion values. After the onset of reperfusion, regional function and myocardial O_2 consumption stabilized at 80 ± 4% [95% confidence interval (CI) 71–89%] and 85 ± 4% (95% CI 75–95%) of preocclusion values.

Hemodynamic and O_2 consumption data in stunned animals are shown in Table 2. During partial occlusion,

Table 1. *Hemodynamic and O_2 consumption data in "hibernating" animals*

	Baseline	Reperfusion (2 h)
Mean Ao pressure, mmHg	87 ± 2.9	89 ± 3.0
Peak Ao pressure, mmHg	103 ± 3.4	101 ± 3.6
Heart rate, beats/min	117 ± 1.7	119 ± 1.9
LV d*P*/d*t*, mmHg/s	1,871 ± 82	1,879 ± 65
Double product × 10^3, mmHg·beats·min^{-1}	11.9 ± 0.38	12.1 ± 0.43
Seg. fx., %		
Test area	14.5 ± 2.7	11.4 ± 1.9*
Remote area	20.2 ± 3.5	20.7 ± 3.0
Test area flow, ml/min	36 ± 4.1	31 ± 2.8
$(A-V)O_2$, ml/100 ml	11.5 ± 0.4	11.1 ± 0.5
$M\dot{V}O_2$, ml/min	4.13 ± 0.6	3.46 ± 0.48*

Values are means ± SE. Ao, aortic; LV, left ventricular; d*P*/d*t*, pressure change over time; Seg. fx., segmental function (systolic segment shortening or wall thickening); $(A-V)O_2$, arterial-venous O_2 difference; $M\dot{V}O_2$, myocardial oxygen consumption. *$P \leq 0.05$ vs. baseline.

Table 2. *Hemodynamic and O_2 consumption data in "stunned" animals*

	Baseline	End *Day 1*	Next Day
Mean Ao pressure, mmHg	94 ± 3.4	90 ± 2.6	87 ± 1.7
Peak Ao pressure, mmHg	108 ± 3.5	104 ± 2.6	101 ± 1.2
Heart rate, beats/min	120 ± 2.5	121 ± 3.1	121 ± 2.9
LV dP/d*t*, mmHg/s	1,795 ± 182	1,904 ± 116	1,733 ± 83
Double product × 10^3, mmHg·beats·min^{-1}	12.9 ± 0.4	12.6 ± 0.4	12.2 ± 0.2
Seg. fx., %			
Test area	17.5 ± 2.8	7.5 ± 1.5*	8.9 ± 2.1*
Remote area	14.9 ± 1.0	15.7 ± 1.5	16.7 ± 1.1
Test area flow, ml/min	33 ± 5.8	43 ± 6.6	36 ± 5.7
$(\dot{A} - V)O_2$, ml/100 ml	10.7 ± 0.4	9.8 ± 0.7*	9.6 ± 0.5*
$M\dot{V}O_2$, ml/min	3.48 ± 0.6	4.12 ± 0.7	3.52 ± 0.6

Values are means ± SE. *$P < 0.05$ vs. baseline.

regional systolic function was reduced to 21 ± 8% of control in animals undergoing reperfusion and to 25–35% of control in animals euthanized without reperfusion. Microsphere flows averaged 39 ± 5% of preocclusion values. During the first hour of reperfusion, regional function and myocardial O_2 consumption stabilized at 40 ± 7% and 123 ± 13% of control. The following day regional function remained depressed, averaging 54 ± 8% (95% CI 35–73%) of preocclusion values, whereas myocardial O_2 consumption was similar to its original values, averaging 105 ± 3% (95% CI 96–114%) of preocclusion levels.

Cardiomyocyte Morphology

Tissue from instrumented sham animals displayed normal myocyte structure (Fig. 1). Myofibrils were preserved in a slightly contracted state with no indication of sarcomeric disruption. Mitochondria showed a densely stained matrix, containing randomly scattered intramitochondrial cation granules. Small quantities of glycogen were located in the perinuclear regions and between neighboring myofibrils. Nuclear chromatin was uniformly dispersed, with only small quantities of

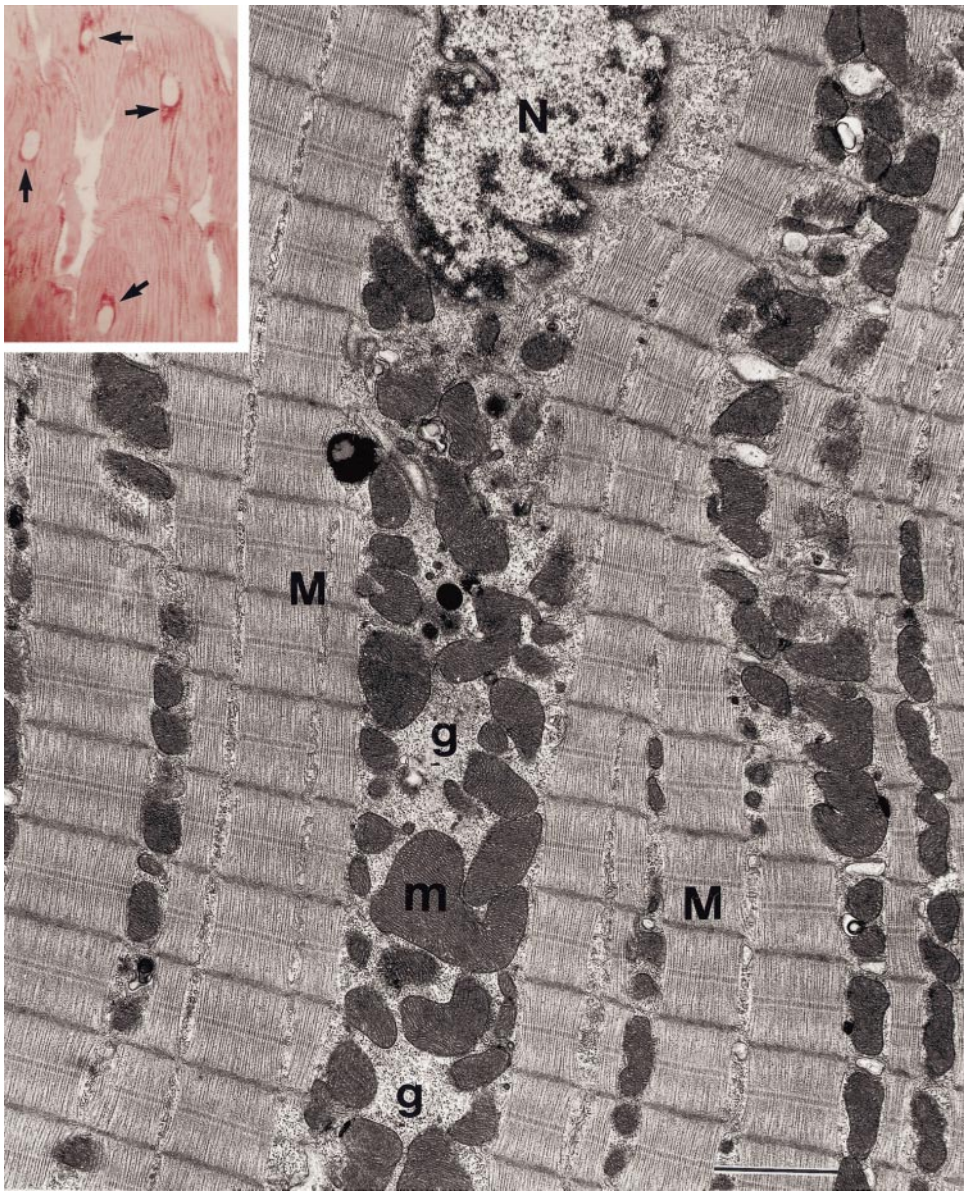

Fig. 1. Fine structure of perinuclear (N) regions of subendocardial cardiac myocytes in a sham animal. Myofibrils (M) are preserved in a contracted state, obliterating most I bands. Small amounts of glycogen (g) are observed in perinuclear areas and between myofibrils. Mitochondria (m) display a condensed matrix possessing intramitochondrial granules. Bar = 2 μm. *Inset*: small amounts of periodic acid-Schiff (PAS)-positive material (*class 1*, arrows) surround myocyte nuclei.

heterochromatin associated with the inner nuclear envelope.

Three novel morphological changes were regularly encountered in myocytes from both experimental models (Figs. 2–7): *1*) myofibrillar disruption, with aberrant arrays of what appear to be thick filaments, developed in perinuclear regions and between adjacent myofibrils of affected cells; *2*) glycogen accumulated in the regions of myocytes displaying myofibrillar disruption; and *3*) myocyte nuclei in cells with disrupted myofibrils frequently displayed clumps of condensed heterochromatin adjacent to, but not coalesced against, the inner nuclear envelope. The pattern of chromatin condensation did not resemble either the margination observed during acute myocardial ischemia (26) or the highly condensed chromatin that becomes segregated against an intact nuclear envelope of apoptotic cells (3, 39). Mitochondrial dilation and/or loss of intramitochondrial matrix was not evident nor was cellular edema or relaxed myofibrils.

These structural changes occurred in both subendocardial and subepicardial tissue but were more prominent in the subendocardium, particularly in the stunning model. They occurred in remote as well as test areas of both experimental models but were more frequent in test areas. Table 3 shows the frequency and degree of myofibrillar disruption in subendocardial myocytes in both models. Disruption was systematically more frequent in stunned than hibernating animals ($P = 0.0002$ by ANOVA) and in test than remote areas of individual animals ($P < 0.0001$). In the hibernation model, disruption was identified in 34 ± 3.8% of myocytes in areas subjected to flow reduction and 16 ± 2.5% of myocytes in remote areas of the same ventricles (Figs. 2 and 4). In stunned animals, disruption was present in 68 ± 5.9% of test areas and 44 ± 7.4% of remote areas (Figs. 3 and 5). In the hibernation model, the frequencies of disruption in test areas were similar in reperfused (31 ± 6.9%) and nonreperfused (37 ± 4.6%) myocytes. In the stunning model, disruption was more frequent in reperfused (74 ± 7.2%) than nonreperfused (47–57%) test areas. *Class 2* disruption (intermyofibrillar as well as perinuclear disruption) was seen most often in stunned reperfused myocytes. *Class 3* disruption (shortened A bands) occurred only in reperfused myocytes and was more frequent in the stunning model. The width of sarcomeric A bands in *class 3* myocytes was reduced (from 1.5 ± 0.1 μm to 0.8 ± 0.2 μm, $n = 50$, $P < 0.01$), whereas Z-Z line dimensions (1.8 ± 0.2 μm) remained unchanged.

Table 3. *Percentage of subendocardial myocytes showing myofibrillar disruption*

	Nonreperfused ($n = 5$)		Reperfused ($n = 7$)	
Class	Test	Remote	Test	Remote
	Hibernation model			
1	21 ± 4.7	16 ± 1.8	23 ± 2.3	10 ± 3.4
2	10 ± 4.2	4 ± 2.1	9 ± 2.0	1 ± 0.9
3	0 ± 0.0	0 ± 0.0	3 ± 1.3	0 ± 0.0
	Nonreperfused ($n = 3$)		Reperfused ($n = 7$)	
Class	Test	Remote	Test	Remote
	Stunned model			
1	42 (37–49)	18 (6–26)	37 ± 5.7	33 ± 4.5
2	11 (5–17)	11 (5–17)	27 ± 5.5	17 ± 4.8
3	0 (0–0)	0 (0–0)	10 ± 3.9	0 ± 0.0

Values are means ± SE or mean (range). Classes of disruption are described in the text.

Because the perinuclear aggregates in disrupted myocytes resembled myosin thick filaments, a monoclonal antibody was employed to localize myosin (12). Both myofibrillar A bands and the filamentous aggregates consistently stained positively with the antimyosin antibody (Fig. 6, *A* and *B*), confirming the presence of the contractile protein in the aggregates. The myosin-positive aggregates displayed no repeating periodicity characteristic of myofibrils (Fig. 6, *A* vs. *B*). In addition, myosin in the A bands of cardiocytes that contained aggregates sometimes appeared to be depleted (Fig. 6*B*).

Table 4 shows the volume densities of intact myofibrils and disrupted thick filament arrays. Values for intact myofibrils were consistently lower in both experimental models than in sham animals. Thick filament arrays were not seen in sham animals and tended to occur more frequently in the stunning model than the hibernation model.

The insets of Figs. 2 and 3 illustrate glycogen accumulation in perinuclear areas of myocytes showing *class 1* and *2* myofibrillar disruption. Figure 7 shows glycogen scores derived from the PAS-stained sections. In both models, glycogen scores were systematically higher in areas subjected to flow reduction than in areas in which flow remained unperturbed.

The pattern of condensed heterochromatin was seen in 46 and 41%, respectively, of subendocardial nuclei from reperfused and nonreperfused hibernation animals, and in 49 and 61%, respectively, of nuclei from reperfused and nonreperfused stunned animals. Ninety percent of all myocytes showing condensed heterochromatin also exhibited myofibrillar disruption.

Small foci of irreversibly injured myocytes were observed in test areas of only two hearts, both of which were from stunned animals that had been reperfused. However, only 1.5% of myocytes in the areas subjected to flow reduction showed such injury. Unlike myocytes showing myofibrillar disruption and glycogen accumulation, these cells consistently displayed mitochondrial osmiophilic densities, glycogen depletion, margination of nuclear chromatin, cellular edema, and sarcolemmal rupture. Their myofibrils showed relaxed I bands consistent with irreversible injury, yet myofibrillar disruption was not apparent.

None of the above-mentioned structural changes were observed in myocytes in the hearts of animals in which euthansia was delayed until segmental function had returned to its baseline level on the day of flow reduction.

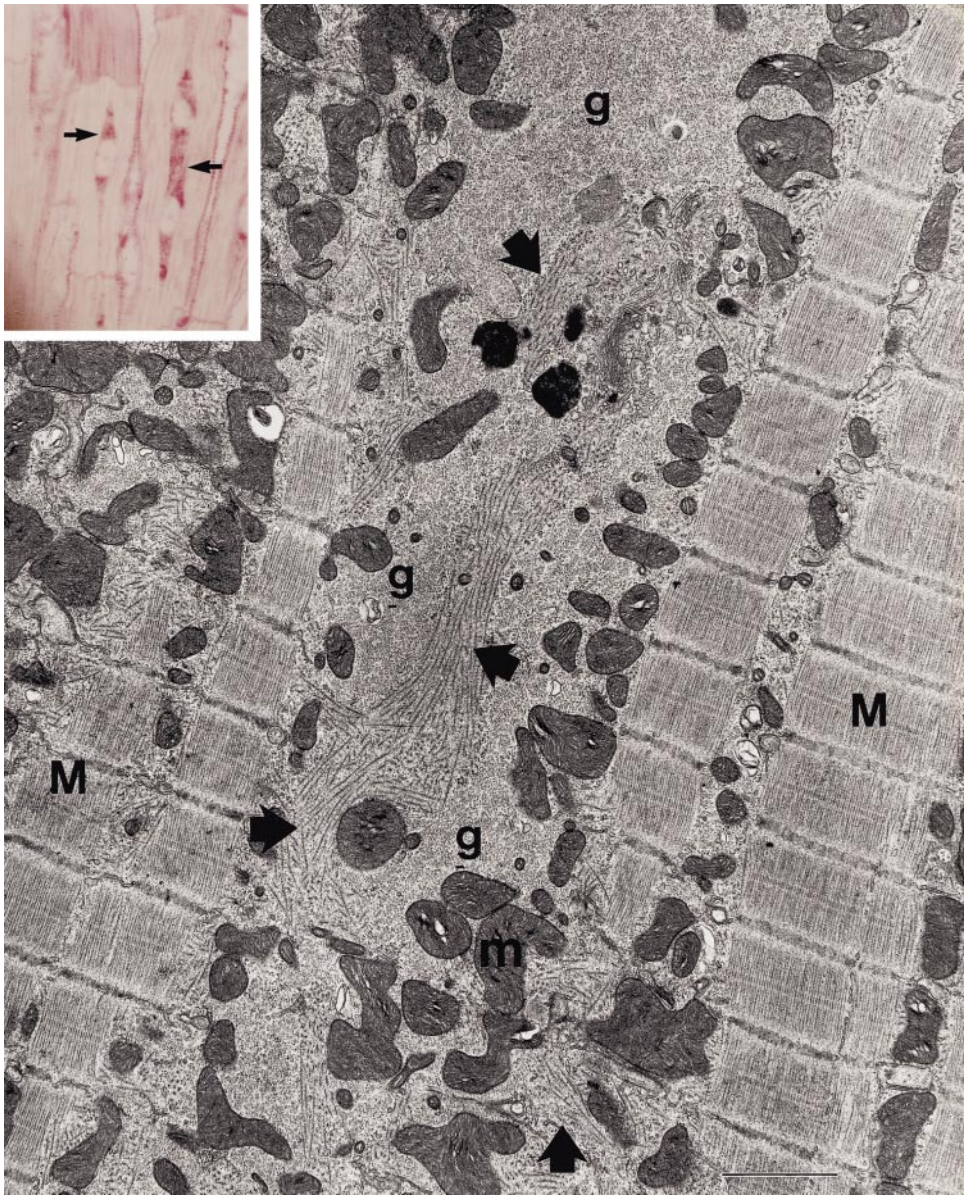

Fig. 2. Ultrastructure in nonreperfused subendocardial myocytes in hibernating model. Perinuclear myofibril disruption (*class 1*, arrowheads) and glycogen accumulation (g) are apparent. Peripheral myofibrillar (M) organization appears normal, as do mitochondria (m). Bar = 2 μm. *Inset*: perinuclear PAS-positive deposits (*class 2*, arrows) are increased.

In Situ End Labeling

Data are presented in Table 5; 0.032% of myocyte nuclei showed in situ end labeling in sham animals. Values in test and remote areas following reperfusion averaged 0.47 ± 0.17% and 0.07 ± 0.06% in the hibernation model ($P = 0.057$) and 0.52 ± 0.20% and 0.15 ± 0.08% in the stunning model ($P = 0.050$). TdT positivity occurred in scattered individual myocytes; clusters of positive cells were not observed.

Although >3,000 nuclei were examined during electron microscopic studies, the pattern of highly condensed chromatin segregated against an intact nuclear membrane characteristic of apoptotic cells was not observed.

Myofibrillar CK Levels

CK activity in myofibrils isolated from areas subjected to flow reduction was reduced systematically in both hibernating and stunned animals (Fig. 8). In the hibernating model, values in the inner ventricular wall and full-thickness myocardium averaged 69 ± 8% (95% CI, 50–88%) and 75 ± 8% (95% CI, 57–93%), respectively, of corresponding values in normally perfused myocardium in the same ventricles. Values in the stunning model averaged 65 ± 8% (95% CI, 47–82%) for the inner ventricular wall and 74 ± 9% for the full-thickness myocardium (95% CI, 54–94%). As shown in Fig. 8, the degree of reduction in CK activity in animals not undergoing reperfusion was similar to that for the entire group in both models.

Troponin I Immunoblotting

No specimen showed a degradation product in the 22- or 26-kDa range with normal loading. With three- to fourfold overloading, test area specimens from two stunned animals showed a faint 26-kDa band. One of

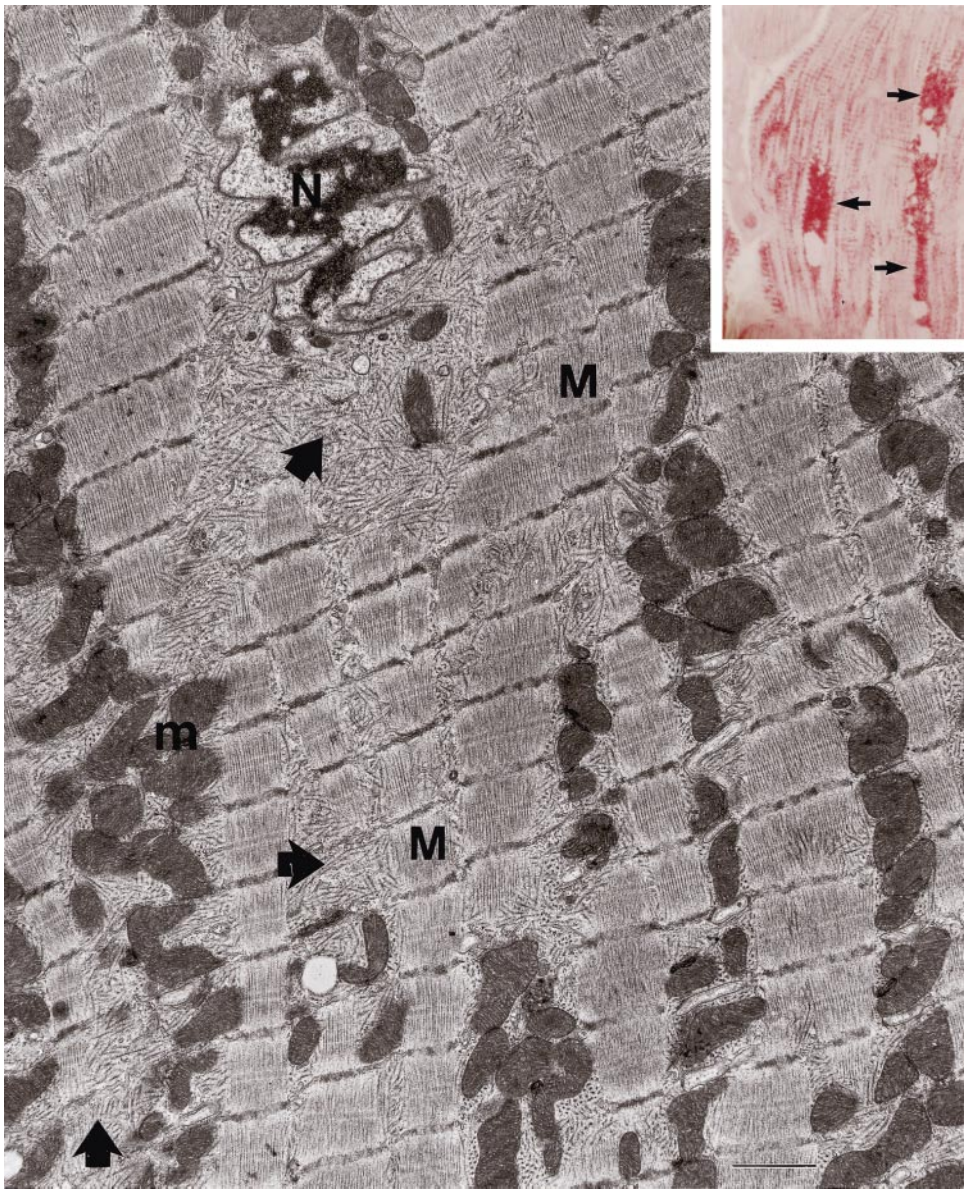

Fig. 3. Ultrastructure in nonreperfused subendocardial myocytes in stunning model. *Class 2* myofibrillar disruption (arrowheads) is apparent in perinuclear (N) area and between myofibrils (M). Disrupted filaments resemble randomly oriented thick filaments. Nuclei (N) display some condensed chromatin, but mitochondrial (m) structure appears unperturbed. Bar = 2 μm. *Inset*: increased perinuclear glycogen deposits (*class 3*, arrows) are apparent.

these animals also showed the electron microscopic foci of irreversibly injured myocytes mentioned above. A representative blot is shown in Fig. 9. Table 6 summarizes results for all animals.

mRNA Levels

α-B-crystallin mRNA in test areas was increased to 145 ± 19% and 159 ± 21% of levels in remote areas in hibernating and stunned animals, respectively (both $P < 0.05$). HSP-70 and HSP-27 mRNAs did not differ significantly in test and remote areas in either the hibernating model (sampled following 2 h of reperfusion) or the stunning model (sampled following 24 h of reperfusion). HSP-70 levels in test areas averaged 133 ± 25% and 121 ± 13% of levels in remote areas. Corresponding values for HSP-27 were 107 ± 23% and 164 ± 34%.

DISCUSSION

The two experimental groups in this study conform to the traditional definitions for hibernation and stunning, i.e., a balanced reduction in systolic function and myocardial O_2 consumption and a persistent reduction in function in the face of normal O_2 consumption. As emphasized by Heusch and colleagues (24, 25), the use of chronically instrumented animals avoids a variety of confounding effects in isolated hearts and acute nonsurvival preparations, which complicate the extrapolation of findings to the usual in vivo situation. Measurements of parameters of injury employed in previous studies help to place the present findings in context. Our electron microscopic observations indicate minimal irreversible injury of myocytes in both experimental models and are consistent with the absence of increased scar tissue noted on quantitative histological

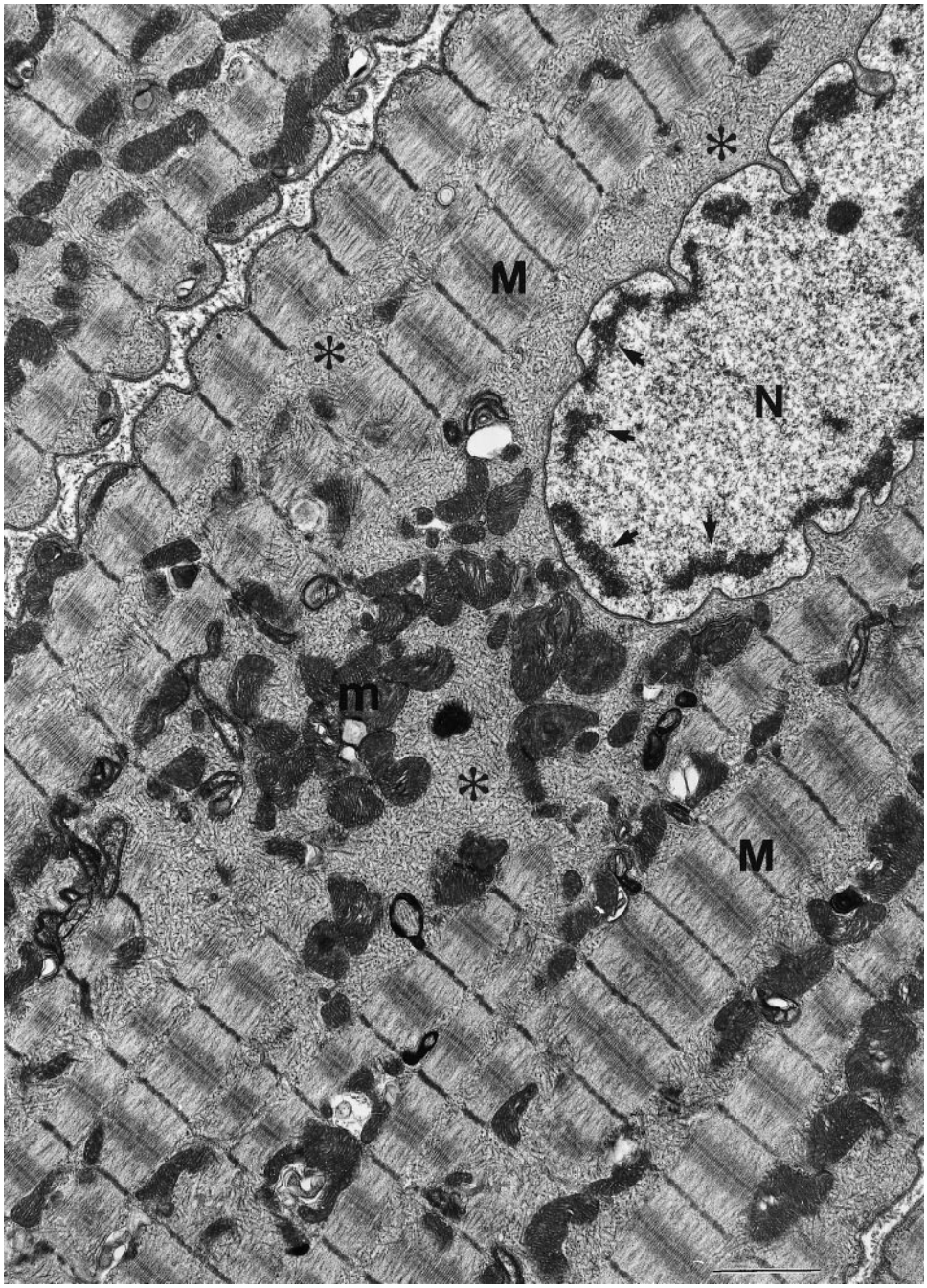

Fig. 4. Ultrastructure reperfused subendocardial myocytes in hibernating model. *Class 3* myofibrillar disruption is characterized by perinuclear (N) and intermyofibrillar thick filament arrays (*) and an apparent reduction in sarcomeric A-band length (M). Distinctive clumping of nuclear chromatin (arrows) is also observed. Mitochondrial (m) matrix remains condensed. Bar = 2 μm.

analysis in an earlier series of animals studied using the same hibernation protocol but euthanized at a later time (50). A minimal extent of cell injury is also suggested by the lack of evidence of troponin I degradation, the modest reduction in myofibrillar CK activity, and the modest increase in mRNA for only one of three stress proteins.

Structural Responses

The consistent disruption of myofibrillar structure observed in both experimental models is, to our knowledge, a new finding. A striking structural feature associated with the disruption of myofibrils was the appearance of aberrant thick filament arrays in the perinuclear regions and between neighboring myofibrils (Figs. 2–5). The mean length and width of these filaments was similar to those of the thick filaments of intact myofibrils, and immunohistochemical staining confirmed the presence of myosin in the arrays (Fig. 6*B*). Thus the irregularly ordered filaments appear to reflect, at least in part, myofibril disassembly.

The occurrence of myofibrillar disruption in areas in which flow remained unperturbed as well as in test areas indicates that the disruption is not solely a result of low-flow ischemia. As shown in Fig. 10, the frequency of disruption, which was systematically greater in test than remote areas, correlated with the degree of end-diastolic lengthening of subendocardial segments during flow reduction in both areas. It is possible that

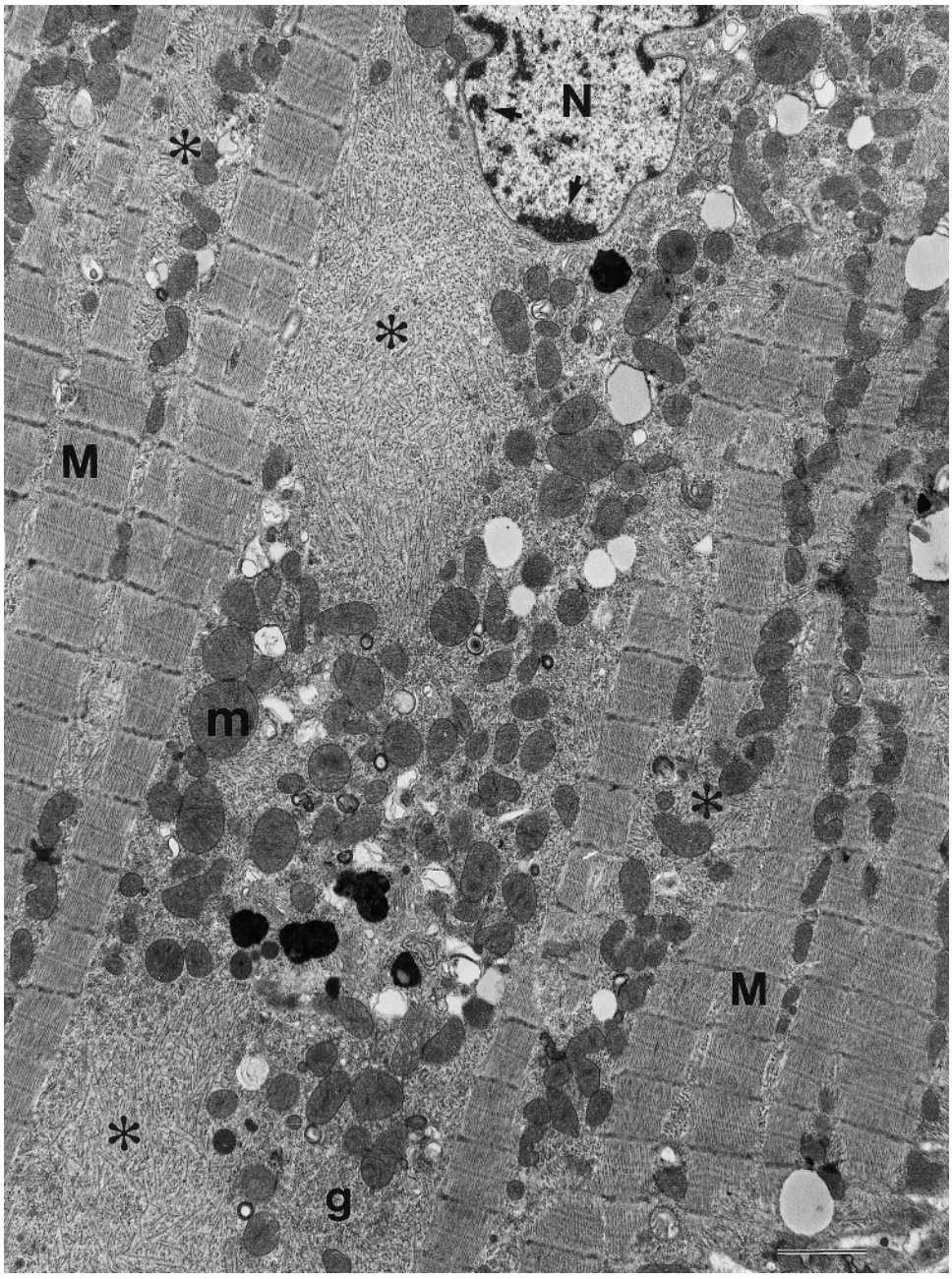

Fig. 5. Ultrastructure in reperfused subendocardial myocytes in stunning model. Perinuclear (N) thick filament aggregates (*) and intermyofibrillar disruption (*) are prominent. Glycogen (g) is also present. Nuclei show small amounts of heterochromatin (arrows). Intact myofibrils (M) and mitochondria (m) retain their normal architecture. Bar = 2 μm.

altered diastolic "stretch" plays a role in myofibrillar disruption. Several in vitro cultured myocyte models have demonstrated a crucial role of mechanical loading in the maintenance of myofibrillar integrity (11, 49). Myofibrillar disassembly in cultured, nonbeating adult heart cells has been characterized by a preferential loss of myosin thick filaments from myofibrils (11). In addition, changes in mechanical loading have been implicated in regulating the expression, synthesis, and degradation of myosin heavy chain (12, 46). Mechanical forces, therefore, appear to have an important role in stabilizing the cardiac myofibril. Alterations in these forces during regional flow reduction could influence the stability of thick filaments, provoking myofibrillar disruption.

The finding of myofibrillar disruption in myocytes from remote as well as test areas may also bear on the ventricular remodeling that follows myocardial injury. Anversa and colleagues have reported that apoptotic cell death occurs in portions of the myocardial wall remote to the site of a myocardial infarction as well as in the infarction itself, in both experimental animals (1) and humans (40). They suggest that this phenomenon results from stretch-mediated release of angiotensin II (29) and that it contributes to dysfunction in the failing human heart (41). In the present study, 90% of the myocytes showing the unusual pattern of condensed nuclear chromatin also showed myofibrillar disruption. The possibility that these findings reflect activation of proapoptotic pathways deserves further study.

The role of myofibrillar disruption in the reductions in segmental function seen in the test areas of both experimental models remains unclear. Because classical stunning can be produced by total occlusions lasting only a few minutes, myofibrillar disruption is unlikely

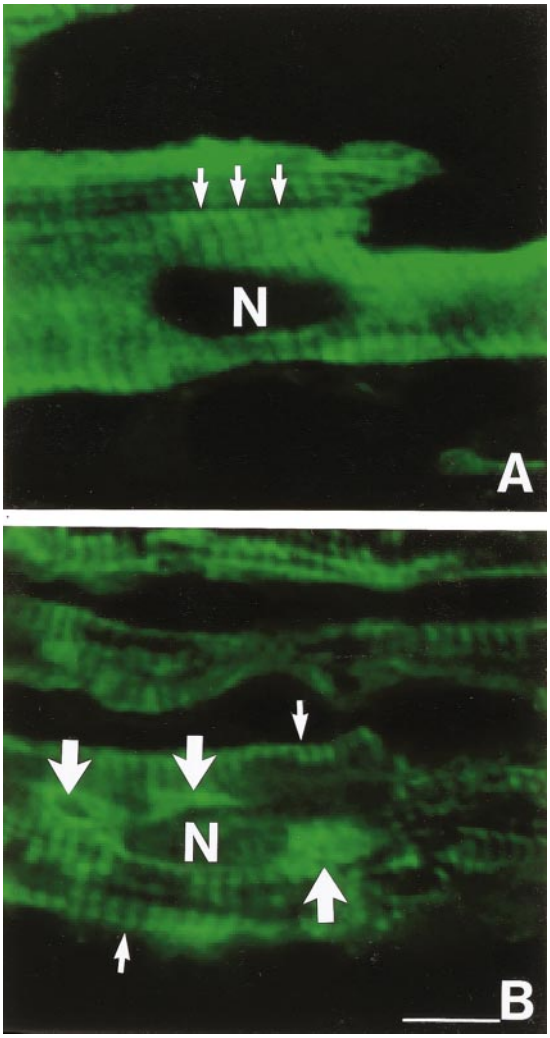

Fig. 6. Distribution of myosin in myocytes from remote (*A*) and reperfused stunned test (*B*) regions of subendocardium. Fluorescence confocal images show the usual A-band staining of normal myofibrils (arrows) in remote myocytes (*A*). In myocytes subjected to flow restriction (*B*), A-band staining is reduced in many sarcomeres (arrows) and perinuclear (N) aggregates of non-myofibrillar myosin (arrowheads) are evident. Bar = 10 μm.

to be the only phenomenon involved. In addition, even though disruption occurred in myocytes from remote as well as test areas, systematic reductions in segmental function were not observed in the remote areas (Tables 1 and 2). Compensatory increases in contractile performance of adjoining "unaffected" myocytes may have counterbalanced in vivo changes in function more effectively in remote than test areas. The fact that disruption was not seen in animals examined after regional function in test areas had returned to normal suggests that the time course of disruption parallels that of reduced function. It also implies that disruption is reversible, at least in the present experimental setting.

Heusch and colleagues (24, 25) have recently summarized animal models previously used to characterize properties of hibernating myocardium. Chen et al. (6) reduced coronary flow to ~60% of baseline for 24 h in porcine hearts. Myofibrillar volume density was reduced at the completion of the 24-h period of reduced flow and returned to normal after 7 days of reperfusion. When a similar degree of flow reduction was applied for 7 days, left ventricular mass increased, possibly in response to an immediate increase in left ventricular volume (7). Although myofibrillar disruption was not reported in either of these studies, it is possible that early myofibrillar disassembly progresses to myofibrillar loss when flow reduction is sustained for a prolonged period and is followed by reactive sarcomeric proliferation.

The systematic increases in glycogen staining in areas subjected to flow reduction in both models seem likely to represent a direct effect of ischemia. Because the elevation in glycogen stores was present in nonreperfused as well as reperfused animals (Fig. 7), it appears to develop rapidly, i.e., within 2 h. As noted above, glycogen accretion has also been noted consistently in human specimens and presumably, represents a chronic as well as acute adaptation. Experimental findings in other laboratories support this view. Increased deposition of ^{18}F-labeled 2-deoxyglucose, presumably representing increased glucose uptake, has been reported in hypoperfused myocardium in chronic porcine models by Fallavollita et al. (14) and McFalls et al. (35). This seems likely to involve translocation of the GLUT4 glucose transporter to the plasma membrane of cardiac myocytes (23, 45, 53). McNulty and Luba (37) report that transient ischemia also leads to an increased regional glucose 6-phosphate concentration followed by a glucose 6-phosphate-mediated increase in the activity of a phosphoprotein phosphatase, which can activate glycogen synthase.

In Situ End Labeling

The degree to which myocyte nuclei from areas subjected to flow reduction show nuclear DNA fragmen-

Table 4. *Volume densities of intact myofibrils and thick filament arrays in cardiomyocytes*

	Intact Myofibrils	Thick Filament Arrays
	Sham Animals (n = 3)	
LCx bed	53 ± 1.4	0
LAD bed	54 ± 1.1	0
	Hibernation model	
Nonreperfused		
Test	46 ± 3.4	6.4 ± 2.1
Remote	50 ± 2.5	3.7 ± 0.9
Reperfused		
Test	46 ± 4.5	11.4 ± 4.4
Remote	47 ± 4.8	4.6 ± 1.3
	Stunned model	
Nonreperfused		
Test	48 ± 2.3	9.2 ± 2.7
Remote	50 ± 1.6	5.1 ± 0.7
Reperfused		
Test	42 ± 3.8	17.9 ± 2.9
Remote	44 ± 2.5	10.6 ± 3.1

Values are means ± SE (in %); n = 3 animals for all groups. LCx, left circumflex; LAD, left anterior descending.

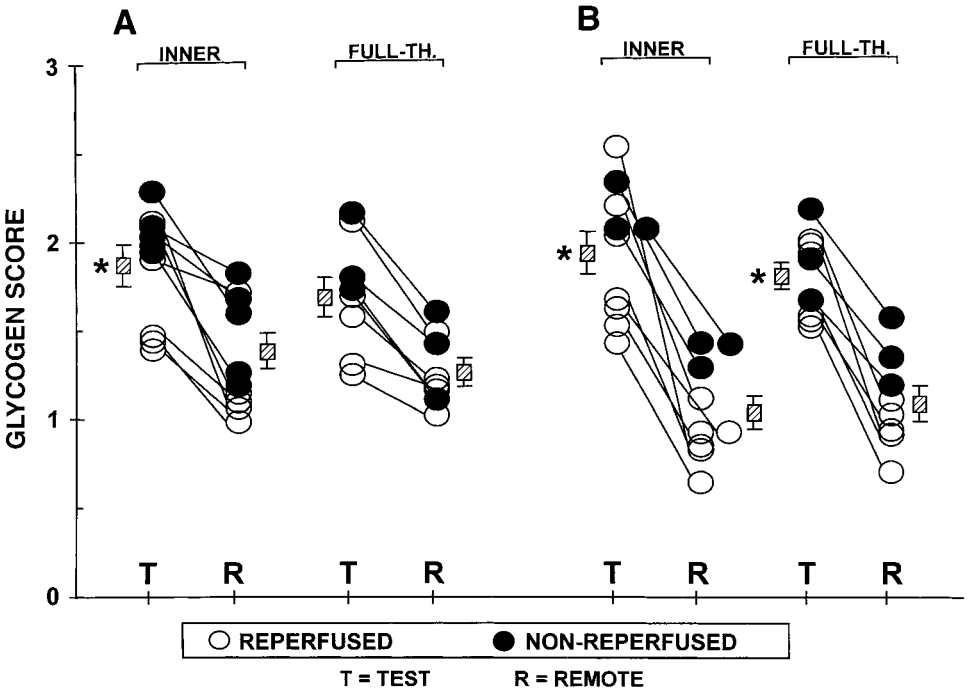

Fig. 7. Glycogen scores in test and remote areas of hibernating (*A*) and stunned (*B*) experimental models. Values are shown for both the inner half of the ventricular wall and the full-thickness wall. *$P < 0.05$.

tation in the present studies is less than in models employing more severe ischemia. The porcine model of Chen et al. (8) shows a systematically greater incidence of TdT-positive nuclei (4.8 ± 2.3%) and a small amount of histological necrosis in the majority of animals. The frequency of DNA fragmentation in frankly infarcted tissue is an order of magnitude larger (18).

In the present experimental models, the frequency of in situ end labeling in reperfused test areas was greater than in remote areas of the same hearts and in sham animals (Table 5). Values in remote areas also tended to be greater than in sham animals, but differences did not reach statistical significance. In the absence of electron microscopic findings characteristic of apoptosis and cellular necrosis, the implications of in situ end labeling in our study remain unclear. As noted previously, further studies will be required to assess the possibility that the unusual nuclear chromatin pattern and myofibrillar disruption we have observed reflect activation of proapoptotic pathways.

Table 5. *Percentage of myocytes showing in situ end labeling*

Sham animals ($n = 3$)	
LCx bed	0.015 ± 0.015
LAD bed	0.049 ± 0.0001
Overall	0.032 ± 0.008
Hibernation model	
Reperfused (2 h) ($n = 7$)	
Test	0.47 ± 0.17
Remote	0.07 ± 0.06
Not reperfused ($n = 3$)	
Test	0.13 ± 0.03
Remote	0.13 ± 0.09
Stunning model	
Reperfused (24 h) ($n = 6$)	
Test	0.52 ± 0.20
Remote	0.15 ± 0.08
Not reperfused ($n = 3$)	
Test	0.30 ± 0.10
Remote	0.03 ± 0.03
After reperfusion and return of function ($n = 3$)	
Test	0.032 ± 0.016
Remote	0.033 ± 0.033

Values are means ± SE; n = number of animals.

Troponin I

Studies in isolated heart preparations have documented troponin I degradation following periods of no-flow ischemia and reperfusion of varying duration (15, 34, 57). Interest has most frequently focused on 22-

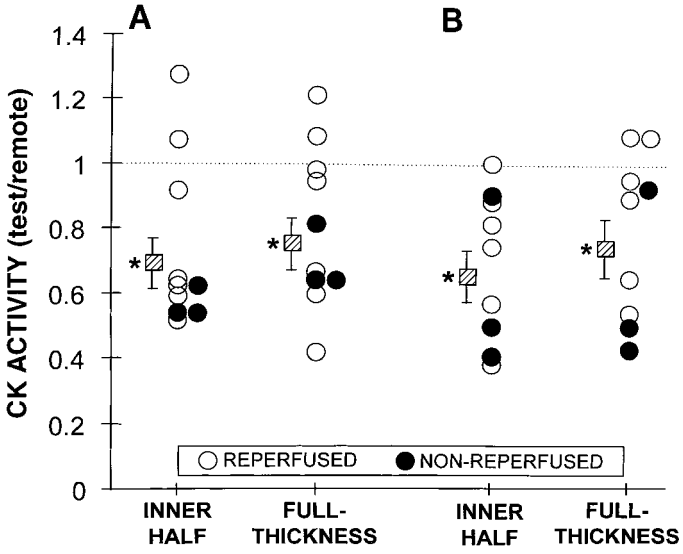

Fig. 8. Myofibrillar creatine kinase (CK) activity in myocardium subjected to flow reduction (test) expressed as a fraction of myofibrillar CK activity in normally perfused myocardium (remote) in the same heart. *A*: hibernating; *B*: stunned. Average values are means ± SE. *95% CI < 1.0.

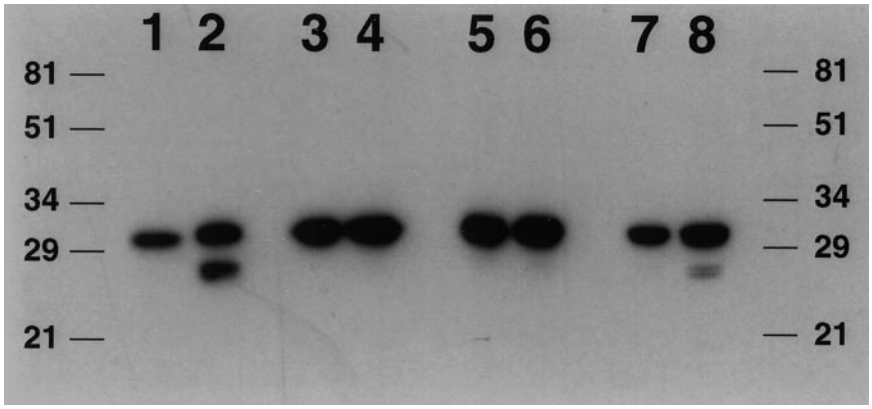

Fig. 9. Immunoblot from a stunned nonreperfused animal. *Lanes 1* and *2* represent negative (pure troponin I) and positive controls (myofibrils incubated with calpain). *Lanes 3* and *4* were loaded with 1.5 and 4.5 μg of protein from remote tissue. *Lanes 5* and *6* were loaded with 1.5 and 4.5 μg of protein from test tissue. *Lanes 7* and *8* are from the same stunned test tissue following incubation with calpain; sample *lane 8* shows a faint 26-kDa band. Densitometric analyses of 26-kDa signals expressed as percentages of 31-kDa signals were 0.5, 39.7, 0.9, 1.1, 1.6, 1.6, 0.0, and 6.1 for *lanes 1–8*, respectively.

to 26-kDa fragments (15, 57), though others have also been identified (34). The infrequent identification of degradation products in the present study corresponds with recent findings in stunned porcine myocardium (33, 55). As noted by Solaro (51), breakdown products have also not yet been identified in human tissue. It is possible that amounts of troponin I breakdown sufficiently small to escape detection in our immunoblotting procedure contributed to the observed reductions in contractile performance (51) or that subtle changes in troponin structure caused significant changes in the troponin regulatory complex without degradation (33). An additional consideration is that irreversible injury can be difficult to avoid in acute isolated heart preparations (55).

Reduced Myofibrillar CK Activity

The reductions in myofibrillar CK activity in situations corresponding to the traditional definitions of both hibernation and stunning indicate that some degree of contractile protein injury occurs commonly during flow reductions that do not produce irreversible myocardial damage. This conclusion is consistent with previous studies of Greenfield and Swain (19) and Hacker and colleagues (20). The former group found myofibrillar CK activity to be reduced by 17% in open-chest dogs 15 min after a 15-min total LAD occlusion. The latter group demonstrated a 33% reduction in myofibrillar CK activity in open-chest pigs following four cycles of a 5-min 60% flow reduction. Although reductions in myofibrillar CK activity could be related to effects of reactive oxygen species and effects on thiol groups (38), they occur in nonreperfused as well as reperfused animals and, as such, cannot be attributed solely to reperfusion-related free radical production.

Even though reductions in myofibrillar CK activity presumably reflect some degree of injury, the partial restoration of function seen immediately after reperfusion in both experimental models indicates that a rapidly reversible downregulation of contractile function also occurs during sustained reductions in flow. Partial restoration of myocardial creatine phosphate

Table 6. *Troponin I immunoblot densitometry: 26-kDa band as percentage of 31-kDa band in overloaded gels*

Sham animal	
LC inner	0.7
LC outer	2.1
LAD inner	0.8
LAD outer	1.3
Hibernation model	
Reperfused (2 h) ($n = 6$)	
Test inner	0.8 ± 0.4
Test outer	0.6 ± 0.4
Remote inner	0.5 ± 0.2
Remote outer	0.5 ± 0.2
Not reperfused ($n = 3$)	
Test inner	1.6 ± 0.4
Test outer	1.5 ± 0.9
Remote inner	1.2 ± 0.2
Remote outer	1.6 ± 0.2
Stunning model	
Reperfused (24 h) ($n = 7$)	
Test inner	1.7 ± 0.7
Test outer	1.4 ± 0.5
Remote inner	1.8 ± 0.6
Remote outer	1.8 ± 0.6
Not reperfused ($n = 3$)	
Test inner	2.4 ± 1.4
Test outer	0.8 ± 0.5
Remote inner	0.9 ± 0.2
Remote outer	1.3 ± 0.3

Values are means ± SE; n = number of animals.

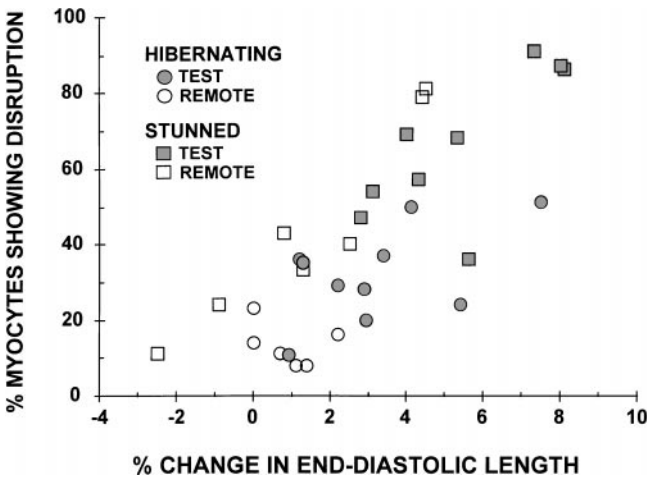

Fig. 10. Frequency of subendocardial myocardial disruption (all classes) is plotted against percent change in end-diastolic subendocardial segment length during the period of flow reduction. Values of end-diastolic length were determined by averaging at least three 30- to 40-s digitized data sets before and during flow reduction. Pearson correlation coefficient is 0.77 ($P < 0.001$). Linear regression is $y = 7.5x + 18$, SEE 16.

levels during sustained flow reductions has been suggested to be one reflection of this downregulation (43, 44, 60), which remains incompletely understood. Kroll et al. (28) recently presented an "open-system kinetics" hypothesis, in which AMP hydrolysis to adenosine and membrane adenosine efflux causes a decrease in the cytosolic concentration of ADP linked to the myokinase reaction. Schaefer et al. (48) suggests that glycolytic production of ATP (as opposed to ATP production by mitochondrial oxidative phosphorylation) is needed for phosphocreatine normalization during sustained low flow ischemia.

The degree to which reductions in myofibrillar CK activity influence reversible postischemic dysfunction remains unsettled. Although marked reductions in total CK activity reduce myocardial contractile reserve (22, 31), normal resting levels of function can be maintained in the face of substantial reductions in total CK (31). At the myofibrillar level, microcompartmentation of CK may play an important role in its functional coupling to myofibrillar ATPase (22, 27, 42, 47). Additional issues relate to possible reductions in the activity of normally functional myofibrillar CK due to limited substrate (ADP) availability (19) and to effects of flow reduction on other myofibrillar components (15).

mRNA Levels

The systematic increase in mRNA for α-B-crystallin in the present hibernation model as well as the stunning model indicates an early response of this, the most abundant cardiac stress protein. The absence of increased levels of HSP-70 mRNA levels is consistent with a preliminary report following an 80-min partial coronary occlusion in anesthetized dogs (21). It is possible that brief total coronary occlusions and more severe degrees of sustained flow reduction are more powerful stimuli for increasing stress protein gene expression than the degrees of flow reduction in the present study (5, 54).

Characterization of Reversibly Hypocontractile Myocardium

Because the present study deals only with short-term changes, its findings cannot be extended to chronic reversible myocardial dysfunction without studies in appropriate animal models and/or patients. Nonetheless, it does demonstrate early myofibrillar disruption and changes in nuclear chromatin pattern in both perfusion-contraction "matches" and "mismatches." A mechanistic characterization of these changes is complicated by their occurrence in remote as well as test ventricular tissue and requires further study. The early increase in glycogen content in both experimental models seems more likely to be an adaptive than injurious response. The reductions in myofibrillar CK activity and modest increases in α-B-crystallin suggest an element of myofibrillar injury in both cases. However, troponin I degradation was not evident in either setting, and, as noted previously, it remains uncertain whether modest reductions in myofibrillar CK activity play a causative role in reduced contractile performance under resting conditions. The similarity of morphological and myofibrillar changes in nonreperfused as well as reperfused animals indicates that these changes also occur during so-called "short-term" hibernation (24).

Although the characterization of reversibly hypocontractile myocardium as hibernating or stunned has been useful in calling attention to beneficial as well as injurious responses to flow reduction, limitations of the dichotomous characterization are recognized. In addition, the terms have sometimes been applied differently by different investigative groups. The overall similarity of responses in our experimental models suggests a similar short-term response complex, including adaptive and injurious components that vary in degree and temporal pattern of expression. The similarity of response bears on the traditional separation of hibernation and stunning on the basis of whether flow and function are reduced "proportionately" or "disproportionately." Reductions in function in either setting have usually been quantified as reductions in regional myocardial shortening or wall thickening. The present observations in the hibernation model confirm an earlier study indicating that modest reductions in perfusion can result in similar percent reductions in myocardial O_2 consumption and regional shortening/thickening following reperfusion (50). More marked reductions in flow in the stunning model are followed by greater percent reductions in regional shortening/thickening than O_2 consumption, thereby meeting the mismatch criterion that has become the sine qua non of stunning. However, studies from at least four laboratories (4, 9, 16, 36, 59) indicate that reperfused stunned myocardium performs more total work in vivo than indicated by measurements of systolic shortening or wall thickening alone. Thus flow and myocardial O_2 demand may sometimes be more appropriately balanced than can easily be appreciated.

The authors gratefully acknowledge the contributions of David Kagan and Wendy Lin in morphological analyses. Dr. Sherman was a Research Fellow of The Thoracic Surgery Foundation for Research and Education.

Address for reprint requests and other correspondence: F. J. Klocke, Feinberg Cardiovascular Research Institute, Tarry 12–703 (T233), Northwestern Univ. Medical School, 303 East Chicago Ave., Chicago, IL 60611-3008 (E-mail: f-klocke@nwu.edu).

Received 1 June 1999; accepted in final form 20 October 1999.

REFERENCES

1. **Anversa P, Cheng W, Liu Y, Leri A, Redaelli G, and Kajstura J.** Apoptosis and myocardial infarction. *Basic Res Cardiol* 93, *Suppl* 3: 8–12, 1998.
2. **Borgers M, Thone F, Wouters L, Ausma J, Shivalkar B, and Flameng W.** Structural correlates of regional myocardial dysfunction in patients with critical coronary artery stenosis: chronic hibernation? *Cardiovasc Pathol* 2: 237–245, 1993.
3. **Buja LM and Entman ML.** Modes of myocardial cell injury and cell death in ischemic heart disease. *Circulation* 98: 1355–1357, 1998.
4. **Buxton DB.** Dysfunction in collateral-dependent myocardium. Hibernation or repetitive stunning? *Circulation* 87: 1756–1758, 1993.
5. **Cave AC, Silverman AS, and Apstein CS.** Ischemic preconditioning does not protect against contractile dysfunction in the

presence of residual flow: studies in the isolated, blood-perfused rat heart. *Circulation* 96: 3087–3093, 1997.
6. **Chen C, Chen L, Fallon JT, Ma L, Li L, Bow L, Knibbs D, McKay R, Gillam LD, and Waters DD.** Functional and structural alterations with 24-h myocardial hibernation and recovery after reperfusion. A pig model of myocardial hibernation. *Circulation* 94: 507–516, 1996.
7. **Chen C, Ma L, Dyckman W, Santos F, Lai T, Gillam LD, and Waters DD.** Left ventricular remodeling in myocardial hibernation. *Circulation* 96: II-46–II-50, 1997.
8. **Chen C, Ma L, Linfert DR, Lai T, Fallon JT, Gillam LD, Waters DD, and Tsongalis GJ.** Myocardial cell death and apoptosis in hibernating myocardium. *J Am Coll Cardiol* 30: 1407–1412, 1997.
9. **Chiu WC, Kedem J, Scholz PM, and Weiss HR.** Regional asynchrony of segmental contraction may explain the "oxygen consumption paradox" in stunned myocardium. *Basic Res Cardiol* 89: 149–162, 1994.
10. **Clark WA, Rudnick SJ, LaPres JJ, Lesch M, and Decker RS.** Hypertrophy of isolated adult feline heart cells following beta-adrenergic-induced beating. *Am J Physiol Cell Physiol* 261: C530–C542, 1991.
11. **Decker ML, Behnke-Barclay M, Cook MG, Lesch M, and Decker RS.** Morphometric evaluation of the contractile apparatus in primary cultures of rabbit cardiac myocytes. *Circ Res* 69: 86–94, 1991.
12. **Decker ML, Janes DM, Barclay MM, Harger L, and Decker RS.** Regulation of adult cardiocyte growth: effects of active and passive mechanical loading. *Am J Physiol Heart Circ Physiol* 272: H2902–H2918, 1997.
13. **Elsasser A, Schlepper M, Klovekorn WP, Cai WJ, Zimmermann R, Muller KD, Strasser R, Kostin S, Gagel C, Munkel B, Schaper W, and Schaper J.** Hibernating myocardium: an incomplete adaptation to ischemia. *Circulation* 96: 2920–2931, 1997.
14. **Fallavollita JA, Perry BJ, and Canty JM, Jr.** 18F-2-deoxyglucose deposition and regional flow in pigs with chronically dysfunctional myocardium. Evidence for transmural variations in chronic hibernating myocardium. *Circulation* 95: 1900–1909, 1997.
15. **Gao WD, Atar D, Liu Y, Perez NG, Murphy AM, and Marban E.** Role of troponin I proteolysis in the pathogenesis of stunned myocardium. *Circ Res* 80: 393–399, 1997.
16. **Gayheart PA, Vinten-Johansen J, Johnston WE, Hester TO, and Cordell AR.** Oxygen requirements of the dyskinetic myocardial segment. *Am J Physiol Heart Circ Physiol* 257: H1184–H1191, 1989.
17. **Glenny RW, Bernard S, and Brinkley M.** Validation of fluorescent-labeled microspheres for measurement of regional organ perfusion. *J Appl Physiol* 74: 2585–2597, 1993.
18. **Gottlieb RA, Burleson KO, Kloner RA, Babior BM, and Engler RL.** Reperfusion injury induces apoptosis in rabbit cardiomyocytes. *J Clin Invest* 94: 1621–1628, 1994.
19. **Greenfield RA and Swain JL.** Disruption of myofibrillar energy use: dual mechanisms that may contribute to postischemic dysfunction in stunned myocardium. *Circ Res* 60: 283–289, 1987.
20. **Hacker TA, Renstrom B, Nellis SH, and Liedtke AJ.** Effect of repetitive stunning on myocardial metabolism in pig hearts. *Am J Physiol Heart Circ Physiol* 273: H1395–H1402, 1997.
21. **Haduczok ZD, Young RF, and Canty JM, Jr.** The relation between transmural perfusion and heat shock protein (HSP-70) expression in canine myocardium (Abstract). *Circulation* 90: I-536, 1994.
22. **Hamman BL, Bittl JA, Jacobus WE, Allen PD, Spencer RS, Tian R, and Ingwall JS.** Inhibition of the creatine kinase reaction decreases the contractile reserve of isolated rat hearts. *Am J Physiol Heart Circ Physiol* 269: H1030–H1036, 1995.
23. **Hashimoto K, Nishimura T, Ishikawa M, Koga K, Mori T, Matsuda S, Hori M, and Kusuoka H.** Enhancement of glucose uptake in stunned myocardium: role of glucose transporter. *Am J Physiol Heart Circ Physiol* 272: H1122–H1130, 1997.
24. **Heusch G.** Hibernating myocardium. *Physiol. Rev* 78: 1055–1085, 1998.
25. **Heusch G, Ferrari R, Hearse DJ, Ruigrok TJC, and Schulz R.** "Myocardial hibernation"–questions and controversies. *Cardiovasc Res* 38: 301–309, 1997.
26. **Jennings RB, Baum JH, and Herdson PB.** Fine structural changes in myocardial ischemic injury. *Arch Pathol* 79: 135–143, 1965.
27. **Krause SM and Jacobus WE.** Specific enhancement of the cardiac myofibrillar ATPase by bound creatine kinase. *J Biol Chem* 267: 2480–2486, 1992.
28. **Kroll K, Kinzie DJ, and Gustafson LA.** Open-system kinetics of myocardial phosphoenergetics during coronary underperfusion. *Am J Physiol Heart Circ Physiol* 272: H2563–H2576, 1997.
29. **Leri A, Claudio PP, Li Q, Wang X, Reiss K, Wang S, Malhotra A, Kajstura J, and Anversa P.** Stretch-mediated release of angiotensin II induces myocyte apoptosis by activating p53 that enhances the local renin-angiotensin system and decreases the Bcl-2-to-Bax protein ratio in the cell. *J Clin Invest* 101: 1326–1342, 1998.
30. **Li XY, McCay PB, Zughaib M, Jeroudi MO, Triana JF, and Bolli R.** Demonstration of free radical generation in the "stunned" myocardium in the conscious dog and identification of major differences between conscious and open-chest dogs. *J Clin Invest* 92: 1025–1041, 1993.
31. **Liao R, Nascimben L, Friedrich J, Gwathmey JK, and Ingwall JS.** Decreased energy reserve in an animal model of dilated cardiomyopathy. Relationship to contractile performance. *Circ Res* 78: 893–902, 1996.
32. **Matsuzaki M, Gallagher KP, Kemper WS, White F, and Ross J, Jr.** Sustained regional dysfunction produced by prolonged coronary stenosis: gradual recovery after reperfusion. *Circulation* 68: 170–182, 1983.
33. **McDonald KS, Moss RL, and Miller WP.** Incorporation of the troponin regulatory complex of postischemic stunned porcine myocardium reduces myofilament calcium sensitivity in rabbit psoas skeletal muscle fibers. *J Mol Cell Cardiol* 30: 285–296, 1998.
34. **McDonough JL, Arrell DK, and Van Eyk JE.** Troponin I degradation and covalent complex formation accompanies myocardial ischemia/reperfusion injury. *Circ Res* 84: 9–20, 1999.
35. **McFalls EO, Baldwin D, Palmer B, Marx D, Jaimes D, and Ward HB.** Regional glucose uptake within hypoperfused swine myocardium as measured by positron emission tomography. *Am J Physiol Heart Circ Physiol* 272: H343–H349, 1997.
36. **McFalls EO, Duncker DJ, Krams R, Sassen LM, Hoogendoorn A, and Verdouw PD.** Recruitment of myocardial work and metabolism in regionally stunned porcine myocardium. *Am J Physiol Heart Circ Physiol* 263: H1724–H1731, 1992.
37. **McNulty PH and Luba MC.** Transient ischemia induces regional myocardial glycogen synthase activation and glycogen synthesis in vivo. *Am J Physiol Heart Circ Physiol* 268: H364–H370, 1995.
38. **Mekhfi H, Veksler V, Mateo P, Maupoil V, Rochette L, and Ventura-Clapier R.** Creatine kinase is the main target of reactive oxygen species in cardiac myofibrils. *Circ Res* 78: 1016–1027, 1996.
39. **Ohno M, Takemura G, Ohno A, Misao J, Hayakawa Y, Minatoguchi S, Fujiwara T, and Fujiwara H.** "Apoptotic" myocytes in infarct areas in rabbit hearts may be oncotic myocytes with DNA fragmentation. *Circulation* 98: 1422–1430, 1998.
40. **Olivetti G, Quaini F, Sala R, Lagrasta C, Corradi D, Bonacina E, Gambert SR, Cigola E, and Anversa P.** Acute myocardial infarction in humans is associated with activation of programmed myocyte cell death in the surviving portion of the heart. *J Mol Cell Cardiol* 28: 2005–2016, 1996.
41. **Olivetti G, Abbi R, Quaini F, Kajstura J, Cheng W, Nitahara JA, Quaini E, Di Loreto C, Beltrami CA, Krajewski S, Reed JC, and Anversa P.** Apoptosis in the failing human heart. *N Engl J Med* 336: 1131–1141, 1997.
42. **Otsu N, Yamaguchi I, Komatsu E, and Miyazawa K.** Changes in creatine kinase M localization in acute ischemic myocardial cells. Immunoelectron microscopic studies. *Circ Res* 73: 935–942, 1993.

43. **Pantely GA and Bristow JD.** Hibernating myocardium: a hypometabolic state for energy conservation. *Basic Res Cardiol* 90: 23–25, 1995.
44. **Pantely GA, Malone SA, Rhen WS, Anselone CG, Arai A, Bristow J, and Bristow JD.** Regeneration of myocardial phosphocreatine in pigs despite continued moderate ischemia. *Circ Res* 67: 1481–1493, 1990.
45. **Russell RRI, Yin R, Caplan MJ, Hu X, Ren J, Shulman GI, Sinusas AJ, and Young LH.** Additive effects of hyperinsulinemia and ischemia on myocardial GLUT1 and GLUT4 translocation in vivo. *Circulation* 98: 2180–2186, 1998.
46. **Samarel AM, Spragia ML, Maloney V, Kamal SA, and Engelmann GL.** Contractile arrest accelerates myosin heavy chain degradation in neonatal rat heart cells. *Am J Physiol Cell Physiol* 263: C642–C652, 1992.
47. **Sata M, Sugiura S, Yamashita H, Momomura S, and Serizawa T.** Coupling between myosin ATPase cycle and creatine kinase cycle facilitates cardiac actomyosin sliding in vitro. A clue to mechanical dysfunction during myocardial ischemia. *Circulation* 93: 310–317, 1996.
48. **Schaefer S, Prussel E, and Carr LJ.** Requirement of glycolytic substrate for metabolic recovery during moderate low flow ischemia. *J Mol Cell Cardiol* 27: 2167–2176, 1995.
49. **Sharp WW, Terracio L, Borg TK, and Samarel AM.** Contractile activity modulates actin synthesis and turnover in cultured neonatal rat heart cells. *Circ Res* 73: 172–183, 1993.
50. **Sherman AJ, Harris KR, Hedjbeli S, Yaroshenko Y, Schafer D, Shroff S, Sung J, and Klocke FJ.** Proportionate reversible decreases in systolic function and myocardial oxygen consumption after modest reductions in coronary flow: hibernation versus stunning. *J Am Coll Cardiol* 29: 1623–1631, 1997.
51. **Solaro RJ.** Troponin I: stunning, hypertrophy, and failure of the heart. *Circ Res* 84: 122–124, 1999.
52. **Solaro RJ, Pang DC, and Briggs FN.** The purification of cardiac myofibrils with Triton X-100. *Biochim Biophys Acta* 245: 259–262, 1971.
53. **Sun D, Nguyen N, DeGrado TR, Schwaiger M, and Brosius FC III.** Ischemia induces translocation of the insulin-responsive glucose transporter GLUT4 to the plasma membrane of cardiac myocytes. *Circulation* 89: 793–798, 1994.
54. **Sun JZ, Tang XL, Knowlton AA, Park SW, Qiu Y, and Bolli R.** Late preconditioning against myocardial stunning. An endogenous protective mechanism that confers resistance to postischemic dysfunction 24 h after brief ischemia in conscious pigs. *J Clin Invest* 95: 388–403, 1995.
55. **Thomas SA, Fallavollita JA, Lee TC, Feng J, and Canty JM Jr.** Absence of troponin I degradation or altered sarcoplasmic reticulum uptake protein expression after reversible ischemia in swine. *Circ Res* 85: 446–456, 1999.
56. **Triana JF, Li XY, Jamaluddin U, Thornby JI, and Bolli R.** Postischemic myocardial "stunning". Identification of major differences between the open-chest and the conscious dog and evaluation of the oxygen radical hypothesis in the conscious dog. *Circ Res* 69: 731–747, 1991.
57. **Van Eyk JE, Powers F, Law W, Larue C, Hodges RS, and Solaro RJ.** Breakdown and release of myofilament proteins during ischemia and ischemia/reperfusion in rat hearts: identification of degradation products and effects on the pCa-force relation. *Circ Res* 82: 261–271, 1998.
58. **Vanoverschelde JL, Wijns W, Borgers M, Heyndrickx G, Depre C, Flameng W, and Melin JA.** Chronic myocardial hibernation in humans. From bedside to bench. *Circulation* 95: 1961–1971, 1997.
59. **Vinten-Johansen J, Gayheart PA, Johnston WE, Julian JS, and Cordell AR.** Regional function, blood flow, and oxygen utilization relations in repetitively occluded-reperfused canine myocardium. *Am J Physiol Heart Circ Physiol* 261: H538–H547, 1991.
60. **Zhang J, Ishibashi Y, Zhang Y, Eijgelshoven MH, Duncker DJ, Merkle H, Bache RJ, Ugurbil K, and From AH.** Myocardial bioenergetics during acute hibernation. *Am J Physiol Heart Circ Physiol* 273: H1452–H1463, 1997.